Ultrafast Dynamics of the $SO_2(H_2O)_n$ Cluster System

T. E. Dermota, D. P. Hydutsky, N. J. Bianco, and A. W. Castleman, Jr.*

Departments of Chemistry and Physics, The Pennsylvania State University, University Park, Pennsylvania 16802

Received: May 13, 2005; In Final Form: July 1, 2005

An investigation of the excited-state dynamics of $SO_2(H_2O)_n$ ($n = 1-5$) clusters following excitation by ultrafast laser pulses to 4.7 eV (coupled $^1A_2$ and $^1B_1$ states) and 9.3 eV (F band) is presented. The findings for the coupled $^1A_2$ and $^1B_1$ states are in good agreement with published computational work[7] and indicate the division of the initial excited-state population into the double well produced by the coupled states. A photoinduced ion-pair formation process is proposed as a likely source of the observed dynamic behavior following the 9.3 eV excitation. Energetics calculations are also presented that support the ion-pair mechanism. A lack of cluster size dependence in the measured time constants indicate surface solvation of SO_2 rather than a cluster structure with the SO_2 molecule fully encompassed by water molecules.

1. Introduction

Interest in the chemistry of SO_2 is wide ranging, from industrial uses to processes of atmospheric significance. The chemistry associated with the tropospheric oxidation of SO_2 to sulfuric acid is significant due to the atmospheric implications of the oxidation process, namely, sulfuric acid's role as a major constituent of acid rain and its involvement in atmospheric nucleation processes. This is especially pertinent considering that the source of SO_2 is primarily anthropogenic, being produced by the combustion of sulfur-containing fossil fuels.[1] On a basic level, the oxidation of SO_2 is thought to proceed by the following steps by either a dry gas-phase mechanism:[2]

$$SO_2(g) + OH(g) \rightarrow\rightarrow\rightarrow SO_3(g)$$

$$SO_3(g) + H_2O(l) \rightarrow\rightarrow\rightarrow H_2SO_4(g)$$

or an aqueous-phase mechanism.

$$SO_2(g) + H_2O(l) \rightarrow H_2SO_3(aq)$$

$$H_2SO_3(aq) + (H_2O_2 \text{ or } O_3)(aq) \rightarrow H_2O(l) + H_2SO_4(aq)$$

On a related note, it has been suggested that SO_2 may react following adsorption on an ice surface to form H_2SO_3.[3,4] This reaction is of interest for two reasons. First, the process leads to the acidification of the ice surface, altering the ice surface chemistry. Second, the now apparently solvated $H^+HSO_3^-$ ions are more strongly bound to the ice surface, decreasing the likelihood of desorption when compared to adsorbed SO_2. The process is likely to influence transport because ice particles are expected to be involved in the movement of molecules from near the earth's surface to the upper troposphere.[3] Tying these two processes together, it seems likely that the ice surface could take the place of liquid water in the aqueous-phase formation of H_2SO_4 in addition to the acidification and transport processes discussed.

Many studies of SO_2 can be found in the literature. A few notable examples are presented here, but the extensive literature on the subject precludes the inclusion of a comprehensive list. Experiments involving resonance enhanced multiphoton ionization (REMPI) studies of the SO_2 monomer[5,6] and dimer[6] have identified the energies of numerous electronic excited states and the accompanying vibrational levels. Computational investigations of the SO_2 potential energy surface[7−9] have elucidated details of SO_2 excited states including energies, coupling processes, and dissociation mechanisms. Experimental investigations from our laboratory have employed the pump−probe dynamics technique[10,11] to monitor the temporal evolution of electronic excited states in the SO_2 molecule,[12] SO_2 clusters,[13,14,41] and $(SO_2)_m(H_2O)_n$[42] clusters. Cluster solvation was found to have substantial influences on the SO_2 electronic excited states under investigation. Therefore, detailed knowledge of molecular SO_2 is insufficient for an understanding of atmospheric chemistry where interaction with and solvation by other molecules is undoubtedly involved in the reactions of interest. Although the specific experimental studies addressed in the present study are not of large significance in the atmosphere, information on the ensuing dynamics is of considerable value in assessing the fate of hydrated species, especially the role of solvation and possibly caging processes. The results presented here are part of our group's ongoing series of experiments devoted to elucidating the photochemistry of neat SO_2 and SO_2 complexes. Further details relating to this study can be found in ref 41.

2. Experimental Methods

The experiments reported herein were performed using the well-established pump−probe technique[10,11] on an instrument composed of an ultrafast laser system coupled to a reflectron[15] time-of-flight mass spectrometer[16] equipped with a pulse-valve cluster source. The laser system[17] consists of a mode-locked Ti:sapphire oscillator (Spectra Physics Tsunami) that generates an 82 MHz pulse train and is pumped by a 10 W argon ion laser (Spectra Physics 2060). Pulse amplification is carried out by a regenerative Ti:sapphire amplifier pumped by the second harmonic of a 10 Hz Nd:YAG laser (Spectra Physics GCR 150−10). For the data reported here, the laser was tuned to ~795 nm, which results in the third harmonic pump and second harmonic probe having wavelengths of ~265 nm and ~398 nm,

10.1021/jp052531l CCC: $30.25
Published on Web 08/27/2005

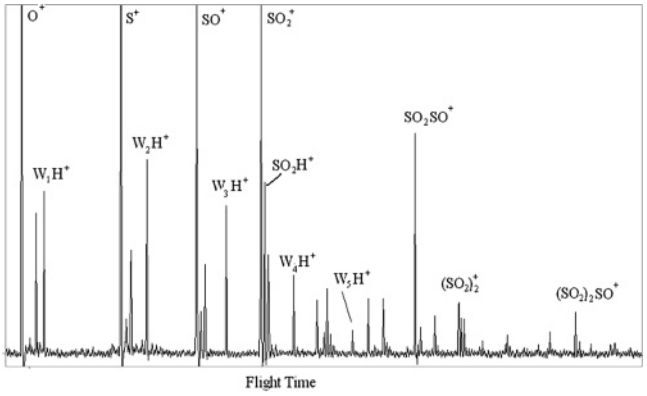

Figure 1. Typical time-of-flight mass spectrum obtained by ionization of the SO_2-H_2O cluster distribution at the temporal overlap of the pump and probe laser pulses. H_2O is represented by W in the mass spectrum.

respectively. The exact values of the wavelengths and laser pulse powers used are presented along with the specific data. SO_2 clusters are generated using a General Valve pulse nozzle[18] via the expansion of a 10% mixture of SO_2 gas diluted in Ar to a total pressure of about 3000 Torr. Water vapor was introduced through the pick-up source[19] to produce mixed clusters by the replacement of SO_2 molecules within neat SO_2 clusters with H_2O molecules. The ion signal generated by the probe pulse was detected by a two plate MCP[20] detector. The signal from the MCP was acquired and averaged by a LeCroy 7200 oscilloscope[21] and then transferred to a PC for analysis. The Delay line[22] that controls the arrival time of the probe pulse and the oscilloscope is controlled by a PC using a program written in LabView.[23] All of the data reported here were taken at pump−probe delay times ranging from −2 ps to either +20 ps or +50 ps, with the range from −2 ps to +2 ps having a data point every 100 fs and the range from +2 ps to +50 having a point every 500 fs. To acquire the data, the average of 20 laser shots was taken at each pump−probe delay time; this process was repeated 5 times and the resulting spectra from these 5 repetitions were averaged together, whereby a total of 100 laser shots were recorded at each delay time. This procedure was employed to reduce the effect any fluctuations in the laser power or the cluster source may have on the data.

3. Results

A $SO_2(H_2O)_n$ cluster mass spectrum typical of that obtained at the overlap of the pump and probe laser pulses is shown in Figure 1. Note the presence of the $(SO_2)_mSO^+$ and protonated water cluster distributions. Protonated water clusters are the ion-state product of $SO_2(H_2O)_n$, as is substantiated and discussed in the text.

A typical pump−probe transient for the $(SO_2)(H_2O)_n$ cluster system is shown in Figure 2 where the points represent the experimental data and the solid line represents the application of a fitting function to that data. Careful analysis of the (SO_2)-$(H_2O)_n$ cluster transients reveals that they consist of three components. The three components can be described as a fast growth followed by a slow decay (dashed line), a fast decay (dotted line), and a constant intensity plateau (dot−dash line). The fitting function I that was used contains a term for each of the three components and is given in eqs 1a−c. In eq 1a: a is the baseline signal intensity (subtracted from the data shown in Figure 2 to bring the baseline of the data to zero), c_1 is the intensity coefficient of the fast rise-slow decay, c_2 is the intensity

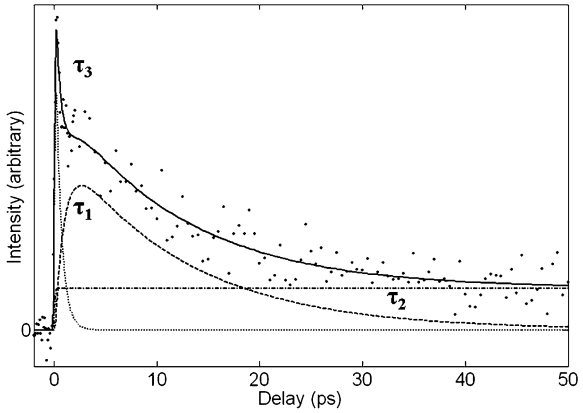

Figure 2. Pump−probe transient of the $(H_2O)_2H^+$ ion signal showing the components of the temporal evolution. Pump: 265 nm, 0.06 mJ/pulse. Probe: 398 nm, 0.23 mJ/pulse.

of the fast decay, and c_p is the intensity of the plateau function (eq 1c).

$$I = a + c_1[I_2(t,\tau_2) - I_1(t,\tau_1)] + c_2[I_3(t,\tau_3)] + c_p[I_p(t)] \quad (1a)$$

The function $I_n(t,\tau_n)$ (eq 1b) was derived in ref 24 and published in the general form used here in ref 25. In this function, σ is the laser pulse width, τ_n is the time constant, t is the pump−probe delay time, and c is an adjustable parameter added to correct for any small variation in the assignment of the $t = 0$ step in the pump−probe transient.

$$I_n(t,\tau_n) = \left[1 - \mathrm{erf}\left\{\frac{\sigma}{2\tau_n} - \frac{t+c}{\sigma}\right\}\right] \exp\left\{\left(\frac{\sigma}{2\tau_n}\right)^2 - \frac{t+c}{\tau_n}\right\} \quad (1b)$$

The constant intensity plateau function (eq 1c) was derived by taking the limit of eq 1b as τ_n goes to infinity to produce a function that can account for the signal intensity in the experimental data that does not evolve on the time scale of the experiment.

$$I_n(t,\tau_n) \xrightarrow[\lim \tau \to \infty]{} I_p(t) = \left[1 - \mathrm{erf}\left\{-\frac{t+c}{\sigma}\right\}\right] \quad (1c)$$

The values of adjustable parameters in eqs 1a−1c were determined by nonlinear regression fitting of the fitting function to the experimental data using Oakdale Engineering DataFit[26] software.

Typical pump−probe transients for the protonated water clusters are shown in Figure 3. The transients consist of the same components indicated in Figure 2. The time constants obtained for the $(H_2O)_nH^+$ cluster series are presented in Table 1. These values are the average of fitting results from seven experiments and the error shown is the standard deviation of those seven values.

The τ_1 and τ_3 components of the $(H_2O)_nH^+$ cluster series transients could not be individually resolved due to the overlap of the two components. The overlap is evident in Figure 2 where the τ_1 growth (dashed line) crosses the τ_3 decay (dotted line) at about 1 ps. As a result, the method that follows was devised to enable the determination of the three time constants. All of the transients were fit using eq 1a with the value of τ_3 fixed at 0.7 ps, enabling the determination of an average value of τ_1 and τ_2 for the seven experiments. Next, the same data were re-fit with τ_1 and τ_2 fixed at the average values to obtain τ_3. Although this method is likely to result in some bias of τ_3 toward 0.7 ps, all other attempts to determine τ_3 were unsuccessful. However, as

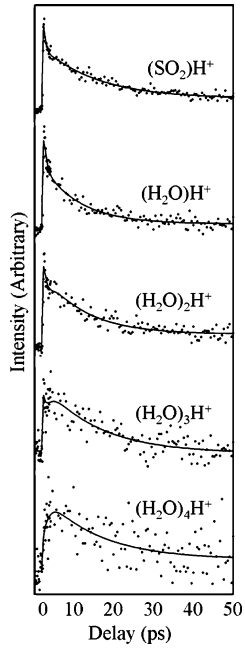

Figure 3. Pump−probe transients of the $(H_2O)_nH^+$ cluster series. Pump: 265 nm, 0.06 mJ/pulse. Probe: 398 nm 0.23 mJ/pulse.

TABLE 1: Average Values of the Three Time Constants Obtained by Fitting Seven Sets of $(H_2O)_nH^+$ Cluster Series Data Obtained with an ~265 nm Pump

	time constants (ps)		
detected ion {predicted neutral}	τ_1	τ_2	τ_3
SO_2H^+ {$SO_2(H_2O)$}	1.5 ± 1.6	12.5 ± 4.9	0.9 ± 0.2
$(H_2O)H^+$ {$SO_2(H_2O)_2$}	0.7 ± 0.5	11.9 ± 3.9	0.7 ± 0.2
$(H_2O)_2H^+$ {$SO_2(H_2O)_3$}	0.9 ± 0.4	12.0 ± 3.7	0.7 ± 0.1
$(H_2O)_3H^+$ {$SO_2(H_2O)_4$}	1.0 ± 0.3	14.2 ± 3.6	0.6 ± 0.3
$(H_2O)_4H^+$ {$SO_2(H_2O)_5$}	1.2 ± 0.4	14.7 ± 5.6	0.8 ± 0.6

can be seen from the values and error bars in Table 1, many of the values obtained deviate from 0.7 ps, leading to the standard deviation of ~±0.2 ps for the τ_3 values. This indicates that during the optimization of the fitting function, τ_3 was able to adjust to values significantly different than 0.7 ps, particularly in the case of the SO_2H^+ species where 0.7 ps is just within the standard deviation of the average value.

4. Discussion

4.1. Ionization Mechanism. The first point that must be explored is the identity of the neutral clusters that lead to the detected ionic products. This is particularly important in the case of clusters containing water, where proton transfer is facile. The second topic of discussion is the mechanism, which accounts for the observed dynamic behavior.

The ion-state products of the mixed $SO_2(H_2O)_n$ clusters can be understood through an analysis of the energetics of the ionization process to determine if ion−molecule reactions and/or evaporation are energetically likely to occur. On the basis of this energy analysis, a reasonable estimate of the neutral cluster size and composition that leads to the observed ion signal can be made. Two energy calculations of cluster signals observed in the mass spectrum and their expected neutral source are given in Table 2. The first calculation indicates the proposed process for the formation of SO_2H^+. It can be seen that the difference between the proton affinities of OH and SO_2 overcomes the smaller difference between the IP's of SO_2 and H_2O. The energy released in the proton-transfer process is probably sufficient to allow the evaporation of the OH fragment which is not detected as part of the cluster. However, if $+A$ is more than 0.53 eV greater than $-A'$, the proton transfer to SO_2 would not be energetically favored. This does not appear to be the case because the SO_2H^+ is observed in the mass spectrum whenever mixed clusters of SO_2 and water are formed. As shown in the second calculation of Table 2, once two water molecules are present in the cluster, the formation of a protonated water molecule is favored because water has a 0.19 eV greater proton affinity then SO_2. As with the mixed dimer, the energy from the ion−molecule reaction is sufficient to evaporate the weakly bound species, namely, SO_2 and OH. As the water cluster becomes larger, the proton affinity of the water portion of the cluster will continue to increase; therefore the proton will reside with the water portion of the cluster at larger cluster sizes. As a result of this energy analysis, it is believed that the SO_2H^+ is the ion-state product of the mixed dimer and the $(H_2O)_{n-1}H^+$ clusters are the ion-state products of $SO_2(H_2O)_n$ with $n > 1$.

TABLE 2: Calculation of the Ion−Molecule Reactions that Are Expected to Lead to the Observed Ion-State Products of $SO_2(H_2O)_n$ Clusters[a]

Ion-State Proton Transfer	
$SO_2^+ \cdot H_2O \rightarrow SO_2^+ + H_2O$	$+A$
$H_2O \rightarrow H_2O^+ + e^-$	$+12.60$[b]
$SO_2^+ + e^- \rightarrow SO_2$	-12.35[c]
$H_2O^+ \rightarrow OH + H^+$	$+6.15$[d]
$SO_2 + H^+ \rightarrow SO_2H^+$	-6.97[d]
$SO_2H^+ + OH \rightarrow SO_2H^+ \cdot OH$	$-A'$
$SO_2^+ \cdot H_2O \rightarrow SO_2H^+ \cdot OH$	$= -0.53$ eV
Dimer Ion-State PT	
$SO_2^+ \cdot (H_2O)_2 \rightarrow SO_2^+ + (H_2O)_2$	$+B$
$(H_2O)_2 \rightarrow 2H_2O$	$+0.12$[e]
$H_2O \rightarrow H_2O^+ + e^-$	$+12.60$[b]
$SO_2^+ + e^- \rightarrow SO_2$	-12.35[c]
$H_2O^+ \rightarrow OH + H^+$	$+6.15$[d]
$H_2O + H^+ \rightarrow H_2OH^+$	-7.16[d]
$H_2OH^+ + SO_2 + OH \rightarrow H_2OH^+ \cdot SO_2 \cdot OH$	$-B'$
$SO_2^+ \cdot (H_2O)_2 \rightarrow H_2OH^+ \cdot SO_2 \cdot OH$	$= -0.64$ eV

[a] The values of A and A' and likewise of B and B' are expected to be similar. The significance of these unknown values is disussed in the text. [b] Reference 27. [c] Reference 28. [d] Reference 29. [e] Reference 30.

Further evidence that the protonated water clusters are the ion-state products of neutral SO_2-containing clusters is found in the observation that the excited-state dynamics of SO_2H^+ and the $(H_2O)_{n-1}H^+$ cluster series (Figure 3) closely resemble each other, indicating that these dynamics involve the excited-state SO_2 chromophore. Therefore, the protonated water clusters must be a product of a neutral cluster containing an SO_2 molecule. An additional piece of evidence related to the observed dynamics is that under the wavelength conditions used, the H_2O^+ signal (not shown) gives rise to a Gaussian-shaped temporal response, having a width that is approximately the temporal width of the laser used. Thus, the long excited-state lifetimes observed for $(H_2O)_nH^+$ are again not likely to be due to excited-state processes of the water molecules.

4.2. Assignment of Transient Components. The observed excited-state temporal evolution following excitation of the SO_2 chromophore within the clusters by the pump laser pulse is found to lead to the formation of two populations of excited-state clusters within the molecular beam sample pulse. An energy diagram is given in Figure 4, which depicts the absorption of one or two pump photons by the SO_2 chromophore and subsequent absorption of three or one probe photons to facilitate ionization. The absorption of one pump photon leads to the excitation of the coupled $^1A_2$ and $^1B_1$ states,[7,31] and the absorption band of SO_2 identified as the F Band[32] is populated by the absorption of two pump photons. As confirmed in the accompanying paper on neat SO_2 clusters by a detailed probe

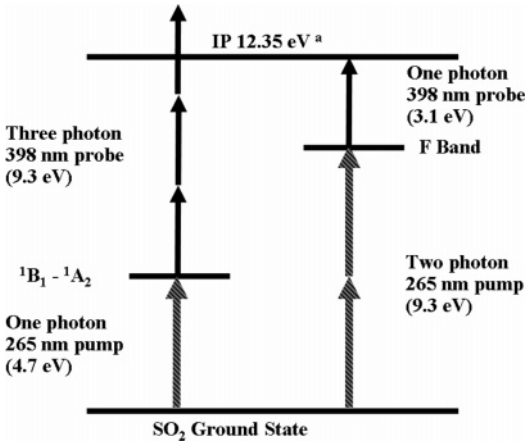

Figure 4. Energy level diagram depicting the generation of excited-state populations in SO_2 by the absorption of one or two pump photons and ionization by probe photons.

laser power dependence study,[41] τ_3 represents the dynamics of the coupled $^1A_2$ and $^1B_1$ states and the τ_1 and τ_2 time constants represent the dynamic behavior that follows the excitation of the SO_2 F band. Unfortunately, attempts to obtain state assignment directly from the $SO_2(H_2O)_n$ data presented here were unsuccessful. However, some qualitative evidence of the state assignment can be seen in Figure 3, leaving little doubt that the state assignments presented above are correct. The "spike" near zero delay time in the pump−probe transients is the τ_3 portion of the data. This spike becomes less prominent relative to the longer time component that is represented by τ_1 and τ_2 as the cluster size increases. It has been clearly observed in our laboratory that the absorption cross section of a cluster decreases as the cluster becomes larger. Three photons of the probe laser are required to ionize a cluster that has been excited by the pump to the coupled $^1A_2$ and $^1B_1$ states. However, only one probe photon is needed to ionize the cluster from the F band. Therefore, as the cluster becomes large (the absorption cross section decreases), the signal from the coupled $^1A_2$ and $^1B_1$ states (three-photon probe) becomes smaller relative to the signal from the F band (one-photon probe) due to the decreasing likelihood of the cluster absorbing three probe photons.

4.3. Interpretation of Time Constant, τ_3. The observed dynamics of the coupled $^1A_2$ and $^1B_1$ states are discussed in the accompanying publication[41] and can be clearly accounted for on the basis of a detailed computational investigation[7] of these coupled states. It has been determined[7] that the initial vertical excitation of the $^1B_1$ state is followed by movement of the excited-state wave packet from the $^1B_1$ state into the double wells that result from the crossing of the $^1A_2$ and $^1B_1$ states. As can be eluded from calculated potential energy surfaces[7−9] of this energy region, the potential energy well minima of both the $^1A_2$ and $^1B_1$ states are likely to be outside of the Franck−Condon region for the absorption of the probe laser pulse. Therefore, ion signal from these states is not observed once the transition has occurred due to ineffective absorption of the probe laser.

On the basis of the above interpretation, the ∼700 fs decay observed for τ_3 is likely to be a measurement of the time needed for the excited-state molecule to pass through the crossing between the initial $^1B_1$ excited state into the $^1A_2$ and $^1B_1$ state minima. Although, this process is reported to proceed rapidly and be complete within 100 fs,[7] the discrepancy between the experimental and computational time constants can be explained. For the signal in the pump−probe experiment to decay, all of the excited-state species must pass through the crossing of the $^1A_2$ and $^1B_1$ states, which requires that the molecules have the correct geometric parameters. This process is likely to be slowed by the excited-state molecules within the ensemble having a variety of geometries depending on each molecule's unique cluster environment. Another factor to consider is that due to the pump wavelength of ∼265 nm used in the experiments reported here, some excess energy is absorbed, putting the chromophore above the $^1A_2$, $^1B_1$ crossing point, which is reported to occur with an excitation of around 300 nm[31,33] above the ground state.

TABLE 3: Energy Calculations of Proposed Neutral Excited-State Ion-Pair Formation Reactions

$SO_2{\cdot}(H_2O) \rightarrow SO_2 + H_2O$	$+A_I$	I
$H_2O \rightarrow H^+ + OH^-$	$+16.92^b$	
$SO_2 + H^+ \rightarrow SO_2H^+$	-6.97^c	
$OH^- + SO_2H^+ \rightarrow OH^-{\cdot}SO_2H^+$	$-B_I$	
$SO_2{\cdot}(H_2O) \rightarrow SO_2H^+{\cdot}OH^-$	= 9.95 eV	
$SO_2{\cdot}(H_2O)_2 \rightarrow SO_2 + (H_2O)_2$	$+A_{II}$	II
$(H_2O)_2 \rightarrow 2H_2O$	$+0.12^f$	
$H_2O \rightarrow H^+ + OH^-$	$+16.92^b$	
$H^+ + H_2O \rightarrow (H_2O)H^+$	-7.16^c	
$SO_2 + (H_2O)H^+ \rightarrow SO_2(H_2O)H^+$	-1.05^d	
$OH^- + SO_2(H_2O)H^+ \rightarrow OH^-{\cdot}SO_2(H_2O)H^+$	$-B_{II}$	
$SO_2{\cdot}(H_2O)_2 \rightarrow SO_2(H_2O)H^+{\cdot}OH^-$	= 8.83 eV	
$SO_2{\cdot}(H_2O)_2 \rightarrow SO_2 + (H_2O)_2$	$+A_{III}$	III
$(H_2O)_2 \rightarrow 2H_2O$	$+0.12^f$	
$H_2O \rightarrow H^+ + OH^-$	$+16.92^b$	
$H^+ + H_2O \rightarrow (H_2O)H^+$	-7.16^c	
$SO_2 + OH^- \rightarrow SO_2{\cdot}OH^-$	-2.68^e	
$(H_2O)H^+ + SO_2OH^- \rightarrow (H_2O)H^+{\cdot}SO_2OH^-$	$-B_{III}$	
$SO_2{\cdot}(H_2O)_2 \rightarrow SO_2OH^-{\cdot}(H_2O)H^+$	=7.20 eV	

[a] Energy calculations of proposed neutral excited-state ion-pair formation reactions. The binding energy values A_x and B_x are not known. [b] Reference 35. [c] Reference 29. [d] Reference 36. [e] Reference 37. [f] Reference 30.

4.4. Interpretation of Time Constant, τ_1. The interpretation of the SO_2 F band dynamics (time constants τ_1 and τ_2) in the water-containing clusters is complex. Some information regarding the states in the F band region of the SO_2 potential energy surface has been found by computational[8] and spectroscopic[44] investigations, which have indicated that this region has a high density of states[8,44] with bound state-like behavior.[44] However, because the properties of this high-energy region of sulfur dioxide's excited-state potential energy surface are not well-known, the proposed dynamics mechanism presented here are based on the observations made in the current experiments. Charge transfer to solvent (CTTS) has been proposed[41] as a mechanism for the dynamics that follow F band excitation in the neat SO_2 cluster system but this cannot be the operative mechanism for water-containing clusters because the electron affinity of water clusters is in the range of 0.2 eV[34] which is insufficient to induce the CTTS process. Therefore, the possibility of an excited-state ion-pair formation process is explored. Three energy calculations are shown in Table 3 for possible ion-pair formation reactions in $SO_2(H_2O)_n$ clusters. Reactions I and II show the formation of SO_2H^+ and $(SO_2)(H_2O)H^+$ within the cluster of SO_2 and one or two water molecules, respectively. Reaction III shows the formation of HSO_3^- within an $SO_2(H_2O)_2$ cluster. The binding energies A_x and B_x are not known. However, one would expect the B_x values to be larger than A_x due to the strength of ionic bonding. Therefore, the calculated values shown are expected to be the upper limit of the energy needed for the processes to take place. Despite the unknown binding energy, the energy needed for either of the clusters containing two water molecules to undergo the ion-pair formation reaction is below the 9 eV pump energy used, making either reaction possible irrespective of the actual value of the binding energy.

The energy obtained for reaction I is greater than the pump energy and would only be spontaneous if B_I is more then 1 eV greater than A_I. Therefore, reaction I cannot be proposed with as much confidence. In light of the energetics of the reactions, excited-state ion-pair formation is proposed as a likely source of the dynamics represented by τ_1 that follow the absorption of two pump photons by the $SO_2(H_2O)_n$ cluster system. This proposed mechanism (particularly reaction III in Table 3) is supported by a recent report that HSO_3^- has been observed to be present within large neutral SO_2−water clusters indicating that under sufficient solvation HSO_3^- formation may be spontaneous in cluster systems.[38] The ion-pair formation mechanism is also supported by the general observation of a dynamic growth in the signal intensity immediately following zero time, which has been observed in our laboratory[39,40] to be indicative of the photoinduced ion-pair formation process.

4.5. Interpretation of Time Constant, τ_2. The question of the source of the slow decay τ_2 remains. Although nothing concrete can be stated, it seems reasonable to suspect the τ_2 decay is the result of a relaxation process within the cluster that follows the proposed photoinduced reactions shown in Table 3. This relaxation process could be in the form of a movement of some of the excited-state population into a lower-lying excited state or simply a decrease in the cluster's ability to absorb the probe laser due to delocalization or dephasing of the excited-state population.

4.6. Cluster Structure. Perhaps the most striking observation relating to the values of τ_1, τ_2, and τ_3 presented in Table 1 is that, within error, each of these time constants is independent of the size of the cluster. It seems that the SO_2 molecule is being solvated by the water molecules in such a way that the addition of more water molecules to the cluster does not lead to any further perturbation of the SO_2 molecule. Computational and experimental studies of small water clusters have shown that the water molecules tend to form ring and chain structures with a coordination number of one or two for each molecule in the cluster.[30,43] Therefore, the water clusters have a two-dimensional structure that may not "enclose" a SO_2 molecule within it. Rather, the SO_2 molecule may reside at the end of a water molecule chain or on the surface of a water molecule ring, in either case having a fairly week interaction with the water cluster. This type of cluster structure would explain the lack of any size dependence in the time constants obtained because the SO_2 molecule in the cluster would only be interacting with a single water molecule no mater what the cluster size.

5. Conclusions

The excited-state dynamics of $SO_2(H_2O)_n$ clusters following excitation by ultrafast laser pulses to 4.7 eV (coupled $^1A_2$, $^1B_1$ states) and 9.3 eV (F band) have been investigated. The findings for the coupled $^1A_2$ and $^1B_1$ states are in good agreement with published computational work.[7] A photoinduced ion-pair formation process is proposed as a likely source of the observed dynamic behavior following the 9.3 eV excitation. Energetics calculations are also presented that support the ion-pair mechanism. The measured time constants lack a cluster size dependence, indicating surface solvation of SO_2 rather than a cluster structure with the SO_2 molecule fully encompassed by water molecules. This finding leads to the suggestion that SO_2 does not become fully solvated to form the HSO_3^- ion until larger clusters than those investigated here are formed. Thus, one would not expect SO_2 to undergo the aqueous-phase conversion to H_2SO_4 on an aerosol particle with a relatively low abundance of water. The studies presented here indicate that SO_2 molecules would be more likely to become weakly adsorbed rather than solvated in a low-water environment.

Acknowledgment. Financial support by the Atmospheric Sciences and Experimental Physical Chemistry Divisions of the U.S. National Science Foundation, Grant No. ATM-0411954, is gratefully acknowledged.

References and Notes

(1) Hewitt, C. N. *Atmos. Environ.* **2001**, *35*, 1155.
(2) Finlayson-Pitts, B. J.; Pitts, N. J., Jr. C*hemistry of the Upper and Lower Atmosphere*; Academic Press: San Diego, 2000.
(3) Clegg, S. M.; Abbott, J. P. D. *J. Phys. Chem. A* **2001**, *105*, 6630.
(4) Abbatt, J. D. P. *Chem. Rev.* **2003**, *103*, 4783.
(5) Xue, B.; Chen, Y.; Hai-Lung Dai. *J. Chem. Phys.* **2000**, *112*, 2210.
(6) Erickson, J.; Ng, C. Y. *J. Chem. Phys.* **1981**, *75*, 1650.
(7) Muller, H.; Koppel, H. *Chem. Phys.* **1994**, *183*, 107.
(8) Kamaya, K.; Matsui, H. *Bul. Chem. Soc. Jpn.* **1991**, *64*, 2792.
(9) Katagiri, H.; Sako, T.; Hishikawa, A.; Yazaki, T.; Onda, K.; Yamanouchi, K.; Yoshino, K. *J. Mol. Struct.* **1997**, *413*, 589.
(10) Zewail, A. H. *Science* **1988**, *242*, 1645.
(11) Zewail, A. H. *J. Phys. Chem. A* **2000**, *104*, 5660.
(12) Knapenberger, Jr., K. L.; Castleman, A. W., Jr. *J. Phys. Chem. A* **2004**, *108*, 9.
(13) Knappenberger, K. L., Jr.; Castleman, A., Jr. W. *J. Chem. Phys.* **2004**, *121*, 3540.
(14) Hurley, S. M.; Dermota, T. E.; Hydutsky, D. P.; Castleman, A. W., Jr. *J. Phys. Chem. A* **2003**, *107*, 3497.
(15) Bergmann, T.; Martin, T. P.; Schaber, H. *Rev. Sci. Instrum.* **1990**, *61*, 2592.
(16) Wiley, W. C.; McLaren, I. H. *Rev. Sci. Instrum.* **1955**, *26*, 1150.
(17) Spectra Physics, 1335 Terra Bella Ave, Mountain View, CA 94039.
(18) General Valve, Parker Hannifin Corp., 19 Gloria Lane, Fairfield, NJ 07004.
(19) Tzeng, W. B.; Wei, S.; Neyer, D. W.; Keesee, R. G.; Castleman, A. W., Jr. *J. Am. Chem. Soc.* **1990**, *112*, 4097.
(20) Burle Electrooptics, Sturbridge Business Park, P.O. Box 1159, Sturbridge, MA 01566.
(21) LeCroy Corp., 690 Chestnut Ridge Rd, Chestnut Ridge, NY 10977.
(22) Aerotech, Inc., 101 Zeta Dr, Pittsburgh, PA 15238-2897.
(23) National Instruments Corp., 11500 N. Mopac Expwy, Austin, TX 78759-3504.
(24) Pedersen, S.; Zewail, A. H. *Mol. Phys.* **1996**, *89*, 1455.
(25) Fiebig, T.; Chachisvilis, M.; Manger, M.; Zewail, A. H.; Douhal, A.; Ochoa, I. G.; De La Hoz Ayuso, A. *J. Phys. Chem. A* **1999**, *103*, 7419.
(26) Oakdale Engineering, 23 Tomey Rd, Oakdale, PA 15071.
(27) Ng, C. Y.; Trevor, D. J.; Tiedemann, P. W.; Ceyer, S. T.; Kronebusch, P. L.; Mahan, B. H.; Lee, Y. T. *J. Chem. Phys.* **1977**, *67*, 4235.
(28) Wang, L.; Lee, Y. T.; Shirley, D. A. *J. Chem. Phys.* **1987**, *87*, 2489. See NIST Web Book.
(29) Hunter, E. P.; Lias, S. G. *J. Phys. Chem. Ref. Data* **1998**, *27*, 413. See NIST Web Book.
(30) Lee, H. M.; Suh, S. B.; Lee, J. Y.; Tarakeshwar, P.; Kim, K. S. *J. Chem. Phys.* **2000**, *112*, 9759.
(31) Heicklen, J.; Kelly, N.; Partymiller, K. *Rev. Chem. Intermed.* **1980**, *3*, 315.
(32) Vuskovic, L.; Trajmar, S. *J. Chem. Phys.* **1982**, *77*, 5436.
(33) Dastareer, A.; Hegazi, E.; Hamdan, A.; Al-Adel, F. *Chem. Phys. Lett.* **1997**, *275*, 283.
(34) Kim, J.; Becker, I.; Cheshnovsky, O.; Johnson, M. A. *Chem. Phys. Lett.* **1998**, *297*, 90.
(35) Smith, J. R.; Kim, J. B.; Lineberger, W. C. *Phys. Rev. A* **1997**, *55*, 2036. See NIST Web Book.
(36) Szulejko, J.; McMahon, T. B. 1992. Personal communication to NIST Web Book.
(37) Squires, R. R. *Int. J. Mass Spectrom. Ion Proc.* **1992**, *117*, 565. See NIST Web Book.
(38) Gridin, V. V.; Geberhardt, C. R.; Tomsic, A.; Schechter, I.; Schroder, H.; Kompa, K. L. *Int. J. Mass Spectrom.* **2004**, *232*, 1.
(39) Hurley, S. M.; Dermota, T. E.; Hydutsky, D. P.; Castleman, A. W., Jr. *Science* **2002**, *298*, 202.
(40) Hurley, S. M.; Dermota, T. E.; Hydutsky, D. P.; Castleman, A. W., Jr. *J. Chem. Phys.* **2003**, *118*, 9272.
(41) Dermota, T. E.; Hydutsky, D. P.; Bianco, N. J.; Castleman, A. W., Jr. *J. Phys. Chem. A* **2005**, *109*, 8259.
(42) Knappenberger, Jr., K. L.; Castleman, A. W., Jr. *J. Chem. Phys.* **2005**, *122*, 154306.
(43) Huneycutt, A. J.; Saykally, R. J. *Science* **2003**, *299*, 1329..
(44) Watkins, I. W. *J. Mol. Spectrosc.* **1969**, *29*, 402.